

The Biphenyl Molecule as a Model Transistor

Paul M. Solomon* and Norton D. Lang*

IBM Thomas J. Watson Research Center, Yorktown Heights, New York 10598

This study is an extension of our previous work,¹ which we will call LS, on charge control in a 4,4'-biphenyl diradical (BPH) molecule linking two electrodes (see Figure 1 for details of structure and definition of terminal voltages), using as before a density-functional treatment with a uniform-background (jellium) model for these electrodes, where the two benzene rings are constrained to be coplanar.^{2–5} This time we examine transport, and the states involved, more closely. Transport is handled very simply in this formulation since wave functions are explicitly available and current densities are derived directly using the quantum mechanical operator. The main thrust of this work is to study the effect of the differing response of the electronic states to the applied field as seen in the electron distributions, and the spatial and energy distribution of the current, as well as effects of the contacts on the state distributions.

Review of Isolated Molecule for Comparison with Transport Calculation. First we discuss an isolated biphenyl molecule (whose rings are

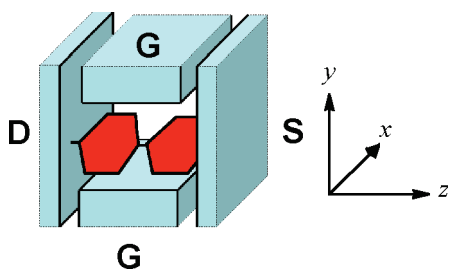


Figure 1. Schematic diagram of our BPH model transistor from ref 1. The benzene rings are constrained to be coplanar, and are oriented at 45° to the y - z plane of the transistor. **G**, **S**, and **D** refer to gate, source, and drain electrodes, respectively, and elsewhere the notation V_G and V_D will refer to the voltages on the gate and drain terminals with the source voltage set at zero. Here *source* refers to the source of electron current.

ABSTRACT We study transport and charge control in a gated 4,4'-biphenyl diradical molecular transistor using self-consistent density-functional calculations. We track both electron-like and hole-like conduction and relate it to the field dependence of current-carrying π -derived states. Owing to the coupling between the two benzene rings, the π -states become segregated into extended, current-carrying states and localized states. Under application of the source/drain field, along the axis of the molecule, the localized π -states become split, while the extended states become polarized and screen the field. The localized states act like isolated islands within the molecule—while they make a substantial contribution to the density of states, they make only a small contribution to transport.

KEYWORDS: molecular transistor · biphenyl · density functional · transport · Lippman-Schwinger · isolated π -state

constrained to be coplanar) with and without a field along the inter-ring axis. (Calculations of free molecular orbitals are done using Gaussian 98.⁶) The purpose is to correlate these well-known results with our calculations for the contacted molecule in order to elucidate the role of the various orbitals in the transport process. Now an isolated benzene ring itself has six π orbitals derived from the carbon 2p states, with the lowest three occupied. The symmetry of the three filled π states⁷ is shown in Figure 2a. We label these states 1, 2, and 3, where 1 is the ground-state and 2 and 3 are degenerate. (It is convenient for our later discussion not to use the usual group-theory designations for these states.) Note that the π states form two groups: full bonding and empty antibonding states. When a biphenyl molecule is created by joining two such rings, each state splits into a pair with bonding and antibonding character, labeled prime (') and double prime (''), respectively (see Figure 2b), but note now that formation of the double ring results in π states that group into those having an extended character (2', 2'') and those having a localized character (3', 3'').⁸ That status may be

*Address correspondence to solomonp@us.ibm.com, langn@us.ibm.com.

Received for review September 24, 2007 and accepted February 12, 2008.

Published online February 27, 2008. 10.1021/nn700253p CCC: \$40.75

© 2008 American Chemical Society

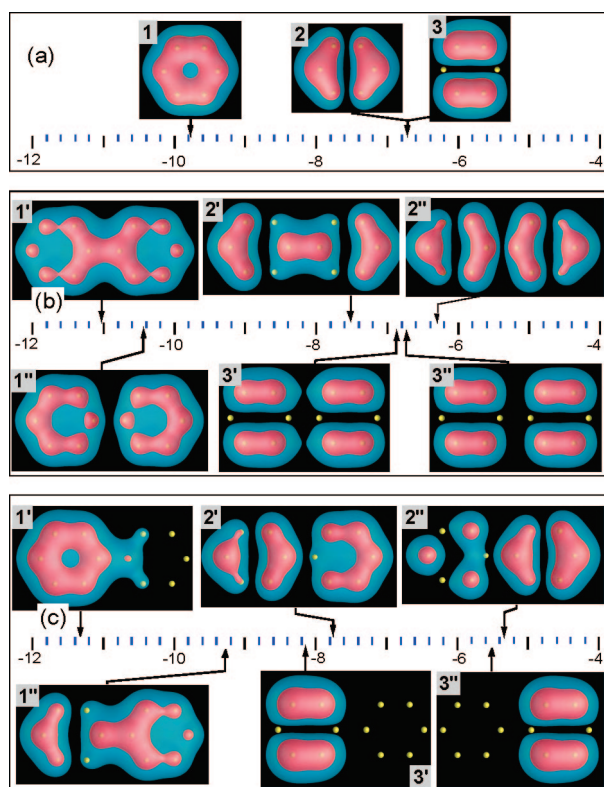


Figure 2. Electron distributions and energies of occupied π states in benzene and the isolated biphenyl molecule computed using the Gaussian 98 program. Two isosurfaces are shown with the outer (transparent) corresponding to $4\times$ lower electron concentration than the inner: (a) the three benzene occupied π states; (b) the six occupied π states of the (constrained planar) biphenyl molecule, with the (') and (") states derived from bonding and antibonding combinations of the three benzene states; (c) the evolution of these states under a field of 0.02 au. The energy scale is in eV.

inferred by the bonding–antibonding energy splitting (see Figure 2b) which is large for states $2', 2''$ (and to a lesser extent for $1', 1''$), indicating strong interaction, but small for $3', 3''$, indicating relative isolation. When a field is applied (Figure 2c) the states $3', 3''$ are strongly split, with each half of the molecule seemingly finding its own potential. On the other hand, the extended states $2'$ and $2''$, which are already split by their interaction, are less sensitive to the field and sense the potential of the whole molecule. As seen in Figure 2c, even though the applied field splits the isolated ($3', 3''$) states apart, it leaves the shape of each half almost unaffected. By contrast, the other, extended, states stay more or less intact, though their shape is strongly polarized by the applied field. Calculations of energies, dipole moments, and the fraction of each state in the two halves of the molecule are shown in Table 1, along with our number classification. We see that the states $3'$ and $3''$ are strongly localized on each half of the molecule. While individual dipole moments are large, the net dipole moment of the pair is small. On the other hand, the other occupied π states are more extended and their shape is strongly affected by the field. They interact with each other electrostatically in such a way

TABLE 1. Properties of the Six Occupied π States of the Isolated Biphenyl Molecule in an Electric Field of 0.02 au Calculated Using Gaussian 98 (ref 6)^a

state ID	level no.	energy (eV)	left (e)	right (e)	dipole moment (au)
1'	29	−11.3	1.92	0.082	8.09
1''	35	−9.23	0.81	1.19	0.14
2'	39	−7.77	1.05	0.95	−0.61
2''	41	−5.34	0.36	1.64	−5.76
3'	36	−8.11	1.99	0.005	8.38
3''	40	−5.53	0.01	1.99	−7.62
net					2.62

^aThe state ID is explained in the text and the level numbers refer to the calculated energy-ordered doubly occupied electronic levels. The net dipole moment shown here is just that of the π states.

that they substantially screen each other and reduce the net dipole moment of the molecule.

Transport Calculation. When the molecule is modeled with contacts (see Theoretical Method section), as in LS (Figure 1), the states are broadened, as shown in Figure 3 for the case of zero source/drain voltage, where the state-identity of a peak is established by correlating the local density of states (LDOS) at the peak energy with the pattern seen in Figure 2b (also identified are some σ states, arbitrarily labeled σ_1 to σ_3). The overall order and energy spacing does indeed carry over from the isolated molecule. Consistent with our picture, the $2', 2''$ (extended) states are broadened considerably more than the $3', 3''$ (localized) π states. We use a different method of analysis when a source/drain voltage of 1.5 V is applied. Instead of looking just at LDOS, we look at LDOS (inc. left) and LDOS (inc. right), the contributions to LDOS from electrons incident from the left- and right-hand contacts, respectively, bearing in mind that the left contact (drain) is at a potential of +1.5 V relative to the right (source). The corresponding total state densities are shown as dashed lines in Figure 4a. We see that the $3''$ and $3'$ states are occupied almost exclusively by electrons incident from the right and left contacts, respectively. The reason is apparent from Figure 4b, where the $3''$ and $3'$ states are each

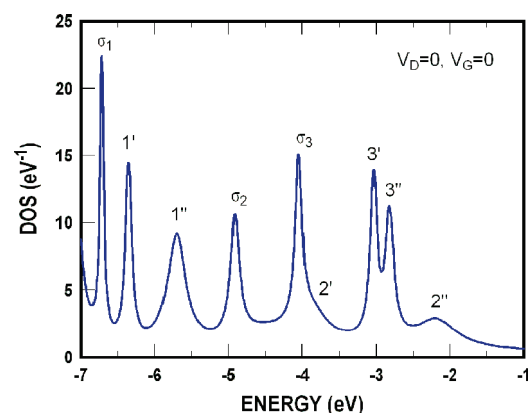


Figure 3. State spectra for a BPH molecule with uniform-background (jellium) contacts, with a source/drain voltage of 0, showing the six occupied π states and several σ states. The Fermi energy is at 0.

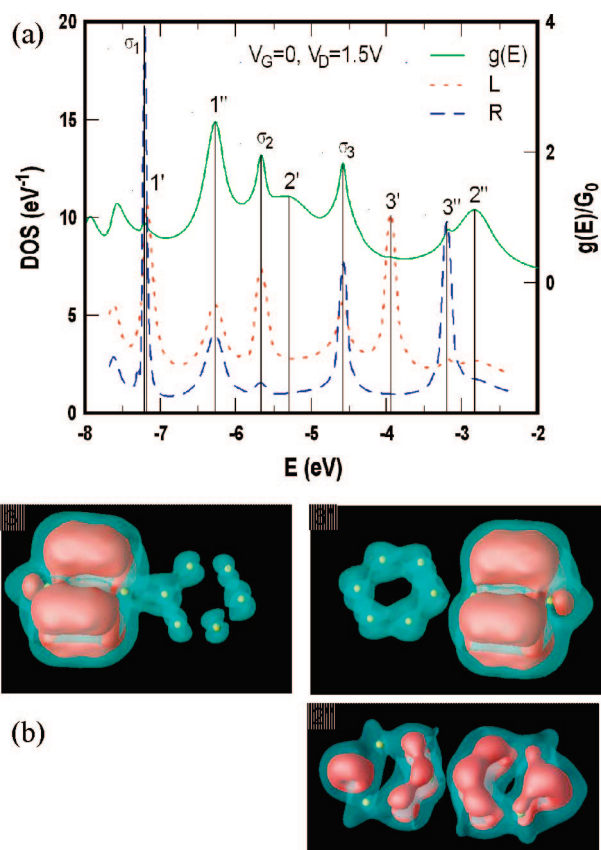


Figure 4. State spectra and LDOS spatial distributions under an applied source/drain voltage of 1.5 V and gate voltage of 0. The two dashed curves are for states populated by electrons originating from the left-hand (L) or right-hand (R) contacts. These curves are offset vertically, by 0.5 and 1.5 units, for clarity. Top curve (right-hand scale) of (a) gives energy-resolved conductance in units of G_0 , the quantum of conductance. Vertical lines are correlated with the state designation marked above, as described in the text. (b) Spatial distributions for the 3' and 3'' and 2'' states.

completely localized on one of the two benzene rings, closely approximating their distribution on isolated benzene molecules. The energy splitting between these states, 0.7 eV, is about half the applied voltage, showing that screening of the field in the direction of the contacts is not very strong. Other states such as 1'' are extended across the whole molecule and can be accessed from either side.

From Figures 2c and 3, the 2' and 2'' states are broadened and extended and should be accessible from both sides of the molecule. They are however strongly masked by the neighboring states so that 2' is all but invisible in the LDOS plots of Figure 4. The 2'' state is seen as a small shoulder in both lower plots of Figure 4a, confirming that it is accessed from both sides. The extended nature of the 2'' state gives it an important role in transport as is shown by plotting the energy density of the quantum mechanical current, originating from the source (upper trace in Figure 4a). While the 3' and 3'' states are barely visible in this trace, the 2''

dominates at higher energies and the 2' state is prominent at lower energies.

Turning our attention to transport, currents⁹ in both n-FET and p-FET modes are shown in Figure 5. The gate voltages are, of course, unrealistic, which is why we call this a “model” transistor, yet we hope that insights gained from this study will aid in real molecular transistor design. To analyze the transport in more detail, we plot, as in Figure 4a (top trace), the current density spectra at gate voltages of -16 , 0 , and 7 V and compare them with the total DOS. The results are shown in Figure 6, solid and dashed traces, respectively (for completeness the lowest unoccupied state, 4', is also shown). It is interesting to trace the evolution of the 3'' state (localized) and the 2'' state (extended). The localized 3'' state moves up more rapidly with decreasing gate voltage than the 2'' state, which is more strongly coupled to the source/drain contacts. At the more positive gate voltage, the 3'' and 2'' states are prominent only in the DOS and conductance spectra, respectively. At the most negative gate voltage (-16 V) the two states tend to merge and state 3'' broadens considerably indicating possible coupling to the contacts *via* state 2''. This is investigated further in the LDOS plots of Figure 7. While still dominated by the characteristic shape of the 3'' state (*cf.* Figure 4b), one observes increased coupling to the right-hand contact at the energy corresponding to the residual 2'' state.

The on-resonance transmission of the extended states approaches unity as shown by the magnitude of the peaks in the $g(E)/G_0$ curves in Figure 6, where numbers greater than unity indicate that current is carried by multiple, or degenerate, states. Also visible in Figure 6 are some of the σ states we identified previously. They are relatively narrow yet have a higher conductance than the 3'' state since a continuous path exists between the source and drain

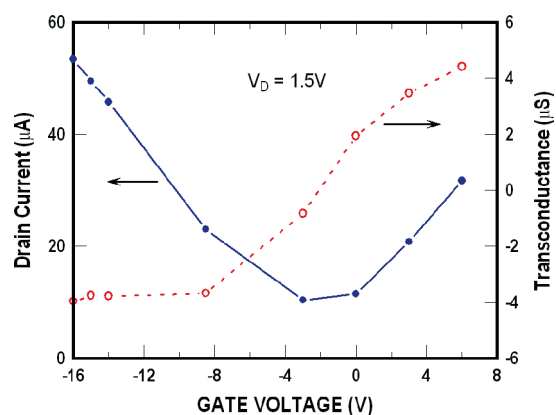


Figure 5. Drain current and transconductance vs gate voltage, at $V_D = 1.5$ V, showing both positive and negative transconductance branches.

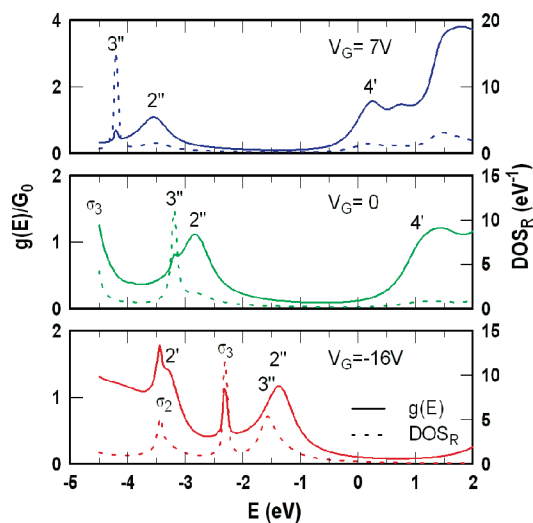


Figure 6. Total DOS spectra compared to conductance (or current density) spectra at $V_G = 7, 0,$ and -16 V, and $V_D = 1.5$ V. Solid curves are conductance, and dashed curves (DOS_R) are local DOS for electrons incident from the right [called DOS (inc. right) in text]. The state designations are discussed in the text.

contacts through these states. For the most negative gate voltage, the conductance of the $3''$ state increases as well, presumably because of coupling *via* the $2''$ state.

Actual current paths can be traced out by plotting streamlines of current flow. Results are shown in Figure 8. Streamlines are initiated at the center of the molecule (see Figure 8b) at an areal density proportional to the local current density, and traced backward and forward to the contacts. The results might at first seem surprising because of the almost complete lack of difference between the current flow in the two halves of

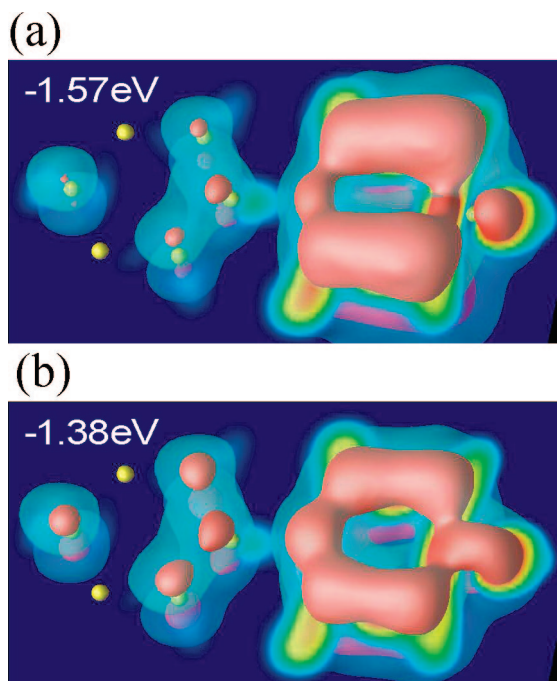


Figure 7. LDOS at marked state energies in Figure 6 for $V_G = -16$ V, (a) at the $3''$ energy, and (b) at the $2''$ energy.

the molecule while the LDOS in the two halves (see e.g., Figure 7a) are so different. However this is largely reconciled by the picture we have developed where at this gate voltage (-16 V) the extended states, which carry most of the current, are largely masked, in the LDOS plots, by the localized $3''$ state. Nevertheless, considering the strong polarization of the extended state $2''$ by the field, it is still somewhat surprising that the current distributions in the two halves should be so similar.

DISCUSSION

In studying this model transistor, some similarities, but several strong departures from conceptual models^{10,11} were found (see Simple Models section for discussion of these models). Previously¹ we had shown that the external gate potential is strongly screened by the σ states. In this study the extended π states polarize as well, yet the polarizations of different states tend to interact and cancel each other. In this work, in contrast to the SK model, where states' contributions to current flow depend only on their width and energy with respect to the source and drain Fermi levels, it is seen that some of the π states are localized and contribute little to the current even at resonance. This could be accounted for in the ZPD model by using very different Γ_1 and Γ_2 terms, which can be justified by observing (see Figure 4) that the $3'$ and $3''$ states, split between the two benzene rings, couple primarily to the same-side contact. Such isolated states, within a conducting band, are typically not found in bulk semiconductors. These "parasitic" states still add to the gate capacitance and thus degrade device performance. Under suitable conditions of gate voltage these states may interact with the contacts *via* extended states at the same energy. This interaction is not ruled out by symmetry considerations since the applied gate and drain fields break the symmetry.

Our work points out the need for caution in deciding which states actually carry current. We see even in this simple model system the emergence of bulk-like semiconductor properties such as band-like conduction, where the HOMO and LUMO levels approximate valence and conduction bands, respectively, yet the existence of isolated states shows that the picture is more complex, and this may perhaps be utilized to obtain interesting new device functionality.

Theoretical Method. The Lippmann–Schwinger equation is solved using a plane-wave basis set, as described in ref 12, for the wave functions of the density-functional formalism whose energies lie between the Fermi levels of the right and left electrodes (in this region only waves incident from one direction are included, which is what gives the net current). In the energy region below the lower Fermi level, the states are treated using a Green's-function method, with an integration around a rectangular contour in the complex

energy plane^{13,14} that extends from below the lowest core-state energy up to the lower Fermi level. Thus if the equation solved for energies between the two Fermi levels is shown symbolically as $\Psi = \Psi_0 + G_0 V \Psi$, the equation solved for energies below the lower Fermi level is $G = G_0 + G_0 V G$, with G_0 being the Green's function for the pair of bare electrodes and G being that for the full system.

Note that the Lippmann–Schwinger equation that in the self-consistent calculation is used only for energies between the source and drain Fermi levels, is also used in a final iteration to get the LDOS over the full energy range. The DOS we consider in this paper is always the difference in density of energy eigenstates between two systems: the electrodes together with the molecule, and the same electrodes (with the same spacing) without the molecule (and without a gate field). The eigenstates are those of the single-particle equations of the density-functional formalism.

Simple Models. In this section we give a brief synopsis of the simple models used in Solomon and Kagan¹⁰ (SK) and Zahid, Paulsson, and Datta¹¹ (ZPD). Both models consider the electrical conduction through a molecule as transmission between source and drain Fermi levels *via* Lorentz-broadened states, with the broadening caused by interaction with the contacts. Both models make the same basic assumptions although the nomenclature is different and this can cause confusion when comparing the two models. ZPD describes a two-terminal model (no gate) where latitude is provided for asymmetric electrostatic coupling of the internal states to source and drain electrodes *via* a parameter η ($0 \leq \eta \leq 1$), where a value of 0.5 gives symmetric coupling. In SK, symmetric electrostatic coupling only is assumed, but the model is three-terminal and the parameter η is used to denote relative coupling of the molecule to the gate *versus* source and drain. The SK model assumes unity transmission at resonance with a molecular state, whereas ZPD has the factor $4\Gamma_1\Gamma_2/(\Gamma_1 + \Gamma_2)^2$, where Γ_1 and Γ_2 give the quantum mechanical coupling of the states to the external reservoirs, which gives the level broadening as $\Gamma_1 + \Gamma_2$. Both models assume ballistic transport and a rigid shift of the resonant levels caused by the drain voltage (ZPD) or by both gate and drain voltage (SK), and the various coupling factors are assumed to be constant, independent of bias. Both models calculate the additional change of the internal potential of the molecule by dividing the change of charge, caused by change of occupancy of the states, by the effective capacitance (assumed constant) to the molecule.

While admittedly crude, the SK model nevertheless exhibits a wealth of behavior from p-channel-like and n-channel-like FET characteristics in the same device, to resonance peaks in the source-drain conductance¹⁵ broadened by space charge effects, as were also shown

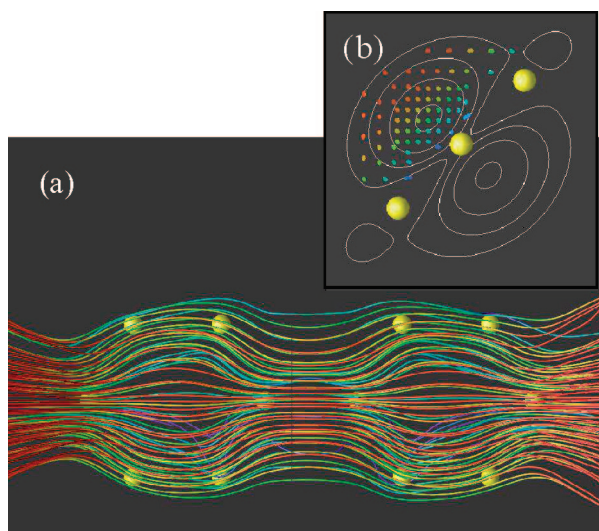


Figure 8. Spatial distribution of the source/drain directed current over a narrow energy range at an energy of -1.48 eV and for a drain voltage of 1.5 V and gate voltage of -16 V. Current streamlines in panel a were derived by originating streamlines from the x - y plane that bisects the molecule at a density proportional to the current density as given by the contours shown in panel b. The colors indicate the distance from the plane of the molecule as seen in panel b.

by ZPD. The purpose of the present paper is in part to investigate how realistic these models are.

REFERENCES AND NOTES

- Lang, N. D.; Solomon, P. M. Charge Control in a Model Biphenyl Molecular Transistor. *Nano Lett.* **2005**, *5*, 921–924.
- It has been shown by Baudour³ that in solid biphenyl, the equilibrium configuration has a twist angle of 13.3° between the two carbon rings, but that at room temperature, the average configuration is planar. For the gas phase, electron diffraction measurements⁴ show a twist angle of 44.4° . The energy difference between a geometry-optimized calculation for the free molecule and a geometry-optimized calculation in which the rings are constrained to be co-planar is 0.09 eV [using Gaussian 98⁶] (*cf.* also ref 5).
- Baudour, J. L. Structural Phase Transitions in Polyphenyls X. Potential Barrier in Crystalline Polyphenyls and in Gaseous Biphenyl Determined Uniquely from Diffraction Data. *Acta Cryst. B* **1991**, *47*, 935–949.
- Almenningen, A.; Bastiansen, O.; Fernholt, L.; Cyvin, B. N.; Cyvin, S. J.; Samdal, S. Structure and Barrier of Internal Rotation of Biphenyl Derivatives in the Gaseous State. Part 1. The Molecular Structure and Normal Coordinate Analysis of Normal Biphenyl and Perdeuterated Biphenyl. *J. Mol. Struct.* **1985**, *128*, 59–76.
- Venkataraman, L.; Klare, J. E.; Nuckolls, C.; Hybertsen, M. S.; Steigerwald, M. L. Dependence of Single-Molecule Junction Conductance on Molecular Conformation. *Nature* **2006**, *442*, 904–907.
- Frisch, M. J.; Trucks, G. W.; Schlegel, H. B.; Scuseria, G. E.; Robb, M. A.; Cheeseman, J. R.; Zakrzewski, V. G.; Montgomery, J. A., Jr.; Stratmann, R. E.; Burant, J. C.; *et al.* *Gaussian 98*, revision A.6; Gaussian, Inc.: Pittsburgh, PA, 1998.
- Jorgensen, W. L.; Salem, L. *The Organic Chemist's Book of Orbitals*; Academic Press: New York, 1973.
- The occupied σ states similarly have extended and localized character which affects their polarizability, but they are sufficiently far below the π states in energy that we will ignore them for the purposes of this paper. They are, of course, part of the calculation.

9. All currents are relative to the current that would flow between the right and left electrodes in the absence of the BPH molecule and the gate.
10. Solomon, P.; Kagan, C. R. Understanding Molecular Transistors. *Future Trends in Microelectronics: The Nano, the Giga, and the Ultra*; Luryi, S., Xu, J., Zaslavsky, A., Eds.; Wiley: New York, 2004; pp 168–180.
11. Zahid, F.; Paulsson, M.; Datta, S. Electrical Conduction Through Molecules. In *Advances in Semiconductors and Organic Nano-Techniques*, Morkoç, H., Ed.; Academic Press: London, 2003; Vol. 3, pp 1–41.
12. Lang, N. D. Resistance of Atomic Wires. *Phys. Rev. B* **1995**, *52*, 5335–5342.
13. Williams, A. R.; Feibelman, P. J.; Lang, N. D. Green's-Function Methods for Electronic-Structure Calculations. *Phys. Rev. B* **1982**, *26*, 5433–5444.
14. Zeller, R.; Deutz, J.; Dederichs, P. H. Application of Complex Energy Integration to Selfconsistent Electronic Structure Calculations. *Solid State Commun.* **1982**, *44*, 993–997.
15. Based on additional simulations using the SK model not included in ref 10.